# IOWA STATE UNIVERSITY
## Digital Repository

2008

# Synthesis and characterization of ionic block copolymer templated calcium phosphate nanocomposites

Mathumai Kanapathipillai
*Ames Laboratory*

Yusuf Yusufoglu
*Iowa State University*, yusufoglu34@yahoo.com

A. Rawal
*Iowa State University*

Y.-Y. Hu
*Ames Laboratory*

C.-T. Lo
*Argonne National Laboratory*

Follow this and additional works at: http://lib.dr.iastate.edu/ameslab_pubs

*See next page for additional authors*

Part of the Chemistry Commons, and the Polymer Science Commons

The complete bibliographic information for this item can be found at http://lib.dr.iastate.edu/ameslab_pubs/242. For information on how to cite this item, please visit http://lib.dr.iastate.edu/howtocite.html.

# Synthesis and characterization of ionic block copolymer templated calcium phosphate nanocomposites

## Abstract

Self-assembling thermo-reversibly gelling anionic and zwitterionic pentablock copolymers were used as templates for precipitation of calcium phosphate nanostructures, controlling their size and ordered structural arrangement. Calcium and phosphate ions were dissolved in a block-copolymer micellar dispersion at low temperatures. Aging at ambient temperature produced inorganic nanoparticles, presumably nucleated by ionic interactions. The self-assembled nanocomposites were characterized by small-angle X-ray and neutron scattering (SAXS/SANS), nuclear magnetic resonance (NMR), thermogravimetric analysis (TGA), and transmission electron microscopy (TEM). 1H-31P NMR with 1H spin diffusion from polymer to phosphate proved the formation of nanocomposites, with inorganic particle sizes from âˆ¼2 nm, characterized by 1H-31P dipolar couplings, to > 100 nm. TEM analysis showed polymer micelles surrounded by calcium phosphate. SAXS attested that a significant fraction of the calcium phosphate was templated by the polymer micelles. SANS data indicated that the order of the polymer was enhanced by the inorganic phase. The nanocomposite gels exhibited higher moduli than the neat polymer gels. The calcium phosphate was characterized by TGA, X-ray diffraction, high-resolution TEM, and various NMR techniques. An unusual crystalline phase with >2 chemically and >3 magnetically inequivalent HPO4 2- ions was observed with the zwitterionic copolymer, highlighting the influence of the polymer on the calcium phosphate crystallization. The inorganic fraction of the nanocomposite was around 30 wt % of the dried hydrogel. Thus, a significant fraction of calcium phosphate has been templated by the tailored self-assembling ionic block copolymers, providing a bottom-up approach to nanocomposite synthesis.

## Keywords

Ambient temperatures, inorganic nano-particles, ionic interactions, low temperatures, pentablock copolymers, phosphate ions, transmission electron ABS resins, block copolymers, calcium calcium alloys, nanocomposites, phosphates, thermogravimetric analysis

## Disciplines

Chemical Engineering | Chemistry | Polymer Science

## Comments

## Authors

Mathumai Kanapathipillai, Yusuf Yusufoglu, A. Rawal, Y.-Y. Hu, C.-T. Lo, Papannan Thiyagarajan, Y. E. Kalay, Mufit Akinc, Surya K. Mallapragada, and Klaus Schmidt-Rohr

# Synthesis and characterization of self-assembled block copolymer templated calcium phosphate nanocomposite gels

D. Enlow,[a] A. Rawal,[b] M. Kanapathipillai,[c] K. Schmidt-Rohr,[b] S. Mallapragada,[c] C.-T. Lo,[d] P. Thiyagarajan[e] and M. Akinc[a]

Self-assembled macroscale calcium phosphate–copolymer nanocomposite gels were prepared using a bottom-up approach from aqueous solutions. Amphiphilic block copolymer micelles in aqueous solutions were used as templates for the growth of calcium phosphate nanocrystals and then allowed to self-assemble in solution to form thermoreversible nanocomposite gels. NMR and XRD showed that calcium phosphate precipitation in a Pluronic® F127 copolymer gel resulted in a disordered brushite phase while the calcium phosphate–poly(2-diethylaminoethyl methacrylate) (PDEAEM) modified Pluronic® F127 pentablock copolymer nanocomposite contained the same brushite phase along with a calcium dihydrogen phosphate second phase. TEM, SAXS, and NMR experiments confirmed that the calcium phosphate precipitated on and interacted with the polymer micelles forming an organized network of ∼20 nm diameter nanospheres. The resulting polymer–calcium phosphate nanocomposite gels contained between 6.5 and 15 weight percent calcium phosphate, which could be controlled by manipulating the pH of the constituent solutions.

## Introduction

In natural bone, nanoscale collagen fibrils act as templates for the nucleation and growth of the calcium phosphate inorganic phase, thereby forming a hierarchically ordered structure with unique properties. In this study, we investigate the formation of bioinspired calcium phosphate nanocomposites on nano-structured self-assembling polymeric micelle templates in solution, which can self-assemble further to form macroscale gels.

Because of their excellent bone biocompatibility, calcium phosphate-based materials and coatings have been studied as potential implant materials. For example, brushite based materials have been developed as bone cements,[1] and biomimetic apatite coatings on titanium have been studied for bone implants.[2,3] Because calcium and phosphate are natural components in bone, many of these materials have improved bone bonding properties.

In an effort to mimic Nature, Muller *et al.* investigated biomimetic apatite formation on chemically modified cellulose templates.[4] After treating highly oriented trimethylsilylether–cellulose (TMS–cellulose) fibers with a supersaturated $Ca(OH)_2$ solution and exposing it to simulated body fluid, Muller *et al.* observed directed calcium phosphate precipitation on the surfaces of the cellulose fibers. Starting with an initial cellulose fiber diameter of about 20 μm, these coated fibers reached a final diameter of over 90 μm. After analyzing the electron diffraction patterns in transmission electron microscopy (TEM), it was found that the calcium phosphate precipitated as both octacalcium phosphate and carbonated hydroxyapatite ($CO_3$-HAp). This was supported by strong calcium and phosphorus signals, and the Ca : P ratio was found to be 1.35 using energy dispersive spectroscopy (EDS). As a mechanism, it was proposed that the chemically-treated active surfaces attracted ions from solution, which initiated precipitation. However, the large initial diameter of the fibers acting as templates did not allow for control of the composite nanostructure.

Similarly, Song *et al.* developed a procedure using poly(2-hydroxyethyl methacrylate) (pHEMA) hydrogel scaffolds.[5,6] Like the cellulose in the previous study, Song *et al.* were able to precipitate calcium phosphate onto the surface of hydrogel strips. In this case, urea was used to slowly raise the solution pH and induce precipitation of calcium phosphate on the carboxylate-rich pHEMA surfaces. The result was a poorly crystalline ∼5 μm thick coating of hydroxyapatite over the surface of the hydrogel strip.

On a smaller length scale, Rusu *et al.* used chitosan as a natural biopolymer matrix for their hydroxyapatite nano-particle composites.[7] By mixing calcium chloride and sodium dihydrogen phosphate with a solution of chitosan in water, they were able to show self-assembly and size control as the hydroxyapatite crystallites formed inside the chitosan matrix. Using this process at 22 °C, the initial product was nearly all brushite. This was converted to hydroxyapatite by raising the pH of the sample to the upper end of hydroxyapatite stability, making brushite a far less stable phase. They held the sample at this high pH and checked the phase with powder X-ray diffraction (XRD) at time intervals from 4 to 24 hours. Hydroxyapatite peaks began to appear immediately after the

*[a]Department of Materials Science and Engineering and Ames Laboratory, Iowa State University, Ames, IA 50011, U. S. A.*
*[b]Department of Chemistry and Ames Laboratory, Iowa State University, Ames, IA 50011, U. S. A.*
*[c]Department of Chemical and Biological Engineering and Ames Laboratory, Iowa State University, Ames, IA 50011, U. S. A.*
*[d]X-Ray Science Division, Advanced Photon Source, Argonne National Laboratory, 9700 South Cass Avenue, Argonne, IL 60439, U. S. A.*
*[e]Intense Pulsed Neutron Source, Argonne National Laboratory, 9700 South Cass Avenue, Argonne, IL 60439, U. S. A.*

pH was raised above 11 and hydroxyapatite was the dominant phase after 24 hours. Using XRD line broadening and TEM analysis, a bimodal crystallite size distribution was observed with 15–20 nm primary crystallites and larger "cluster-like" domains of 200–400 nm.

While all of these studies produced biomimetic polymer–ceramic composites, the polymer–ceramic interaction was limited mostly to the surface of the bulk polymer or the polymer micelles. With a similar process using copolymer micelles that self-assemble to form a gel, our approach involves precipitating calcium phosphate onto the copolymer micelles and having them self-assemble to form a network of agglomerated polymer–inorganic nanospheres, a model for a bottom-up approach to the design of nanocomposites.

The Pluronic® F127 block copolymer, poly(ethylene oxide)-b-poly(propylene oxide)-b-poly(ethylene oxide) (PEO-PPO-PEO) and the poly(2-diethylaminoethyl methacrylate, PDEAEM) modified Pluronic® F127 pentablock copolymer (PDEAEM-b-PEO-b-PPO-b-PEO-b-PDEAEM) developed by Determan et al.[8] self-assemble into micelles at low temperature and concentration in aqueous solutions. These micelles entangle to form viscous gels at higher temperatures or concentrations, typically above 25 °C.[9] The temperature-dependent phase transformation of the copolymers allows mixing of the solutions of copolymer and inorganic constituents followed by formation of a homogeneous mixture of the micelle spheres and calcium phosphate by manipulating the temperature and/or pH of the solution. While previous studies were limited to calcium phosphate–polymer interaction on the surface of a bulk polymer, or agglomerates of nanocomposites at the sub-micro scale from solution, these polymers make it possible to precipitate calcium phosphate in the interstitial spaces between and on the surfaces of the concentrated spherical micelles within a macro-scale copolymer gel formed completely by self-assembly. The Pluronic® F127 is uncharged and the pentablock copolymers are charged at low pH, so the effect of surface charge on the formation of the inorganic phase was also investigated.

## Experimental

### Materials and methods

Unless otherwise noted, all chemicals in this study were obtained from Fisher Scientific and are of laboratory grade and purity. Precipitation of calcium phosphate into the copolymer gel matrix was achieved using aqueous solutions of ammonium dihydrogen phosphate ($NH_4H_2PO_4$), phosphoric acid ($H_3PO_4$), calcium nitrate ($Ca(NO_3)_2$) and the Pluronic® or PDEAEM pentablock copolymers. A saturated solution of calcium phosphate with a Ca : P ratio of 1.67 as in stoichiometric hydroxyapatite was prepared by mixing 120 mL of a 0.5 M solution of ammonium $NH_4H_2PO_4$ with 200 mL of a 0.5 M $Ca(NO_3)_2$ solution. This solution was stirred for 30 minutes until a white precipitate formed. The mixture was then centrifuged and the clear supernatant was drawn off as the saturated calcium phosphate solution. This supernatant solution had a pH of 3.0.

A more concentrated solution was prepared by mixing 4.0 M solutions of $H_3PO_4$ and $Ca(NO_3)_2$. NaOH was added until the solution reached a pH of 1.0 and a cloudy precipitate formed. Like the dilute solution described above, the supernatant was saved as the saturated calcium phosphate solution at pH = 1.0.

Commercially-available Pluronic® F127 (BASF Corporation, Florham Park, New Jersey) ($M_n$ = 12 600, 70% PEO) and the modified $PDEAEM_{35}$-F127-$PDEAEM_{35}$ pentablock copolymer developed by Determan et al.[8] were used as the polymer matrix phase. Gel samples were prepared by dissolving 3 g of the copolymer directly into the calcium phosphate solutions. Control samples of the copolymer dissolved in deionized water were also prepared. These mixtures were placed in a refrigerator at 3 °C and stirred daily until the copolymer was completely dissolved. It took usually about 3 to 4 days to get a homogeneous solution. After dissolving, the samples were warmed to room temperature (22 °C) and aged for 24 hours. During this time, as predicted by the temperature/concentration phase diagram, the calcium phosphate–copolymer solution thickened into a viscous nanocomposite gel.

In order to analyze the growth of the ceramic coatings on the micelles, a less-concentrated 0.5 wt% polymer solution (below the critical gel concentration) was also tested. To prepare this sample, 10 mL of the pH 3.0 calcium phosphate solution was mixed with an equal amount of 1.0 wt% pentablock copolymer solution yielding a solution of 0.5 wt% pentablock copolymer, and half of the saturated calcium phosphate ion concentration. This solution was placed in a 25 °C temperature-controlled water bath, and allowed to age. Samples were taken after 30 min, 1 h, 24 h, and after two weeks for TEM observation. Micrographs of the 24 h and the two-week samples were indistinguishable, implying that the system reached apparent equilibrium within the first 24 hours.

### Characterization methods

Transmission electron microscopy (TEM) was used to directly visualize the nanostructure of the gels. Because it was important to retain and analyze the solution structure of the copolymer micelle or gel, cryogenic TEM was necessary. To prepare the TEM samples of the copolymer solutions, 50 μL of the aqueous sample was placed onto a Formvar coated copper grid for 1 min, allowing the contents to settle. Most of the supernatant was wicked away and 1% phosphotungstic acid (pH 6.2) was applied for 30 s as a negative contrast stain. The grid was wicked and allowed to dry. Images were captured on a JEOL 1200EX II scanning transmission electron microscope (Japan Electron Optic Laboratories, Peabody, MA) using a Megaview III digital camera and SIS Pro. software (Soft Imaging Systems Inc., LLC, Lakewood, CO).

Gel samples were prepared as described above, placed onto a bulls-eye stub, and frozen at −100 °C in the chamber of a Reichert Ultracut S ultramicrotome with FCS cryo unit (Mager Scientific Inc., Dexter, MI). Sections were made using a Diatome cryo-diamond knife (35°-dry Electron Microscopy Sciences, Ft. Washington, PA) at 100 nm and collected onto 300 mesh copper grids and placed into a grid transfer unit stored in liquid nitrogen until transferred to the TEM chamber. TEM samples were loaded into a liquid nitrogen cooled Gatan cold stage (Model 626DH, Gatan Inc. Pleasanton, CA) and imaged at 100 kV in a Phillips CM 30

TEM (Phillips Corporation, Schaumburg, IL). Qualitative chemical analysis was done with a ThermoNoran EDS unit calibrated to its internal standards (Thermo Electron Corporation, Waltham, MA).

Small angle X-ray scattering (SAXS) experiments were performed on the Pluronic® F127 and pentablock copolymer gels with and without the inorganic phase using the instrument at the 12-ID beam line at the Advanced Photon Source in Argonne National Laboratory to elucidate the gel nanostructure. A 15 × 15 cm detector was used to measure the scattered intensity and the transmitted intensity was measured using a photodiode. Samples were held in DSC pans for solids, 2 m from the detector. The beam energy used for the analysis is 12 keV ($\lambda$ = 1.035 Å) and the data were collected at 1 s exposures. The collected 2D data was corrected and azimuthally averaged.

Crystalline phases were identified by X-ray diffraction, using a $\theta$–$\theta$ X-ray diffractometer (Scintag, XGEN-400, Cupertino, CA). Wet gel samples were placed in an amorphous polymer sample holder and analyzed immediately to minimize drying. The Cu K$\alpha$ X-ray source was set to 45 kV and 40 mA, and the samples were scanned at a rate of $1° \text{ min}^{-1}$ over a 2$\theta$ range of 10–70°. Phase analysis was done using the ICDD database and the Scintag DMSNT search/match software.

Thermogravimetric analysis (TGA) was performed with a Perkin Elmer thermogravimetric analyzer (Perkin Elmer, TGA 7, Downers Grove, IL) to obtain the fraction of the inorganic phase. Approximately 40 mg of the gel sample was placed in a platinum pan and the experiments were performed in a flowing air environment. The program was set to heat up to 100 °C and hold at this temperature for 10 min, then heat from 100 to 150 °C at a rate of 3 °C $\text{min}^{-1}$, and finally heat from 150 to 800 °C at a rate of 10 °C $\text{min}^{-1}$.

Solid-state NMR can provide useful information about the composition of the calcium phosphate and about the proximity of organic and inorganic components, *i.e.* about the size of the nanostructures formed. The presence of water in solid-state NMR samples is undesirable since ionic currents lead to dissipation of radio-frequency power and can cause broadening of the probe-head tuning curve as well as sample heating. To prevent this, the samples were first dried by rotary evaporation and then lyophilized. For magic-angle-spinning NMR experiments, the samples were packed into 2.5-mm zirconia rotors with Kel-F caps. As desired, the probe head-tuning curve showed no significant broadening and the $^1$H NMR spectrum was free of signals of loosely bound water.

All NMR experiments were carried out on a Bruker spectrometer (Bruker-Biospin DSX400, Rheinstetten, Germany) at 400 MHz for $^1$H and 162 MHz for $^{31}$P nuclei. A Bruker 2.5 mm double resonance magic-angle spinning (MAS) probehead, which enables short $^1$H and $^{31}$P pulse lengths of 2.5 μs duration for a 90° flip angle, was used for 6.5 kHz MAS $^1$H–$^{31}$P experiments. In direct-polarization (DP) $^{31}$P experiments, recycle delays of 400 and 1000 s were used. In $^1$H and $^1$H–$^{31}$P cross-polarization (CP) experiments, including two-dimensional (2D) $^1$H–$^{31}$P wideline separation (WISE), recycle delays of 2 s were used before 400 μs of Hartmann–Hahn cross-polarization (CP). The $t_1$ increment was 20 μs. Due to the presence of sharp peaks in the $^1$H spectrum, both cosine- and sine-modulated data were acquired to give the full frequency information in the $^1$H dimension.

Direct polarization (DP) and cross polarization (CP) $^{31}$P NMR spectra were acquired with $^1$H decoupling at 6.5 kHz MAS. The DP spectrum is quantitative if the recycle delay is sufficiently long. In order to ensure this, the DP experiments were run with increasing recycle delays until there was no further increase in signal intensity. $^1$H–$^{31}$P CP experiments indicate the protonation state of the phosphate group, most pronouncedly after a short (<500 μs) cross-polarization time. The comparison with the DP spectrum indicates whether there are non-protonated phosphates present, which cross polarize slowly or not at all. No Hahn spin echoes were used before detection because the transverse relaxation time of $^{31}$P in one sample (Pluronic®-based composite) was extremely short, possibly due to unfavorable proton dynamics in the phosphate.

All $^1$H NMR spectra were recorded at 6.5 kHz MAS using probe-head background suppression.[10] The line-width of the proton spectrum indicates the $^1$H–$^1$H dipolar coupling, which increases with the proton density and decreases with the mobility of the segment. In rigid organic solids, the dipolar line width is ~40 kHz.

Supramolecular proximities and domain sizes can be probed in NMR using $^1$H proton spin diffusion, during a "mixing" time $t_m$ on the ms to 0.5-s time scale. During the evolution period of a two-dimensional experiment, the magnetization of protons in one phase (*A*) is modulated by its characteristic chemical-shift frequency $\omega_A$. If during $t_m$ the magnetization diffuses to protons in a different phase (B), it will be detected with frequency $\omega B$; thus, domain proximity on the spin diffusion length scale (0.5–30 nm, depending on $t_m$) results in an ($\omega_A$, $\omega_B$) cross peak in the two-dimensional spectrum. For small domain sizes, the equilibration is a fast process, while it is relatively slow for large domains. In the present case, phosphate protons are only a small percentage of the protons in the sample and, therefore, difficult to detect. Hence, we detect them indirectly, with excellent selectivity, in terms of $^{31}$P spins to which these protons cross-polarize.

The experiment with $^1$H evolution flanked by excitation and z-storage 90° pulses, spin diffusion time $t_m$, read-out pulse, cross polarization to $^{31}$P, and $^{31}$P detection effectively is a 2D WISE experiment.[11] At short $t_m$, the slice along the $^1$H dimension will reflect only the phosphate protons near the detected $^{31}$P spins; at longer $t_m$ times, if there is spin diffusion contact between the phosphate protons and the protons from the surrounding polymer matrix, the $^1$H line shape will change to that of the polymer protons. This approach was previously demonstrated in polymer–clay nanocomposites using $^1$H–$^{29}$Si WISE NMR by Hou *et al.*[12]

## Results and discussion

### Supramolecular structure

Transmission electron microscopy of the pentablock copolymer micelles in deionized water in dilute aqueous solutions is consistent with cryo-TEM analysis done by Determan *et al.*,[8] who observed 60–90 nm diameter spheres in a 3 wt% pentablock micelle solution. A TEM micrograph of the polymer
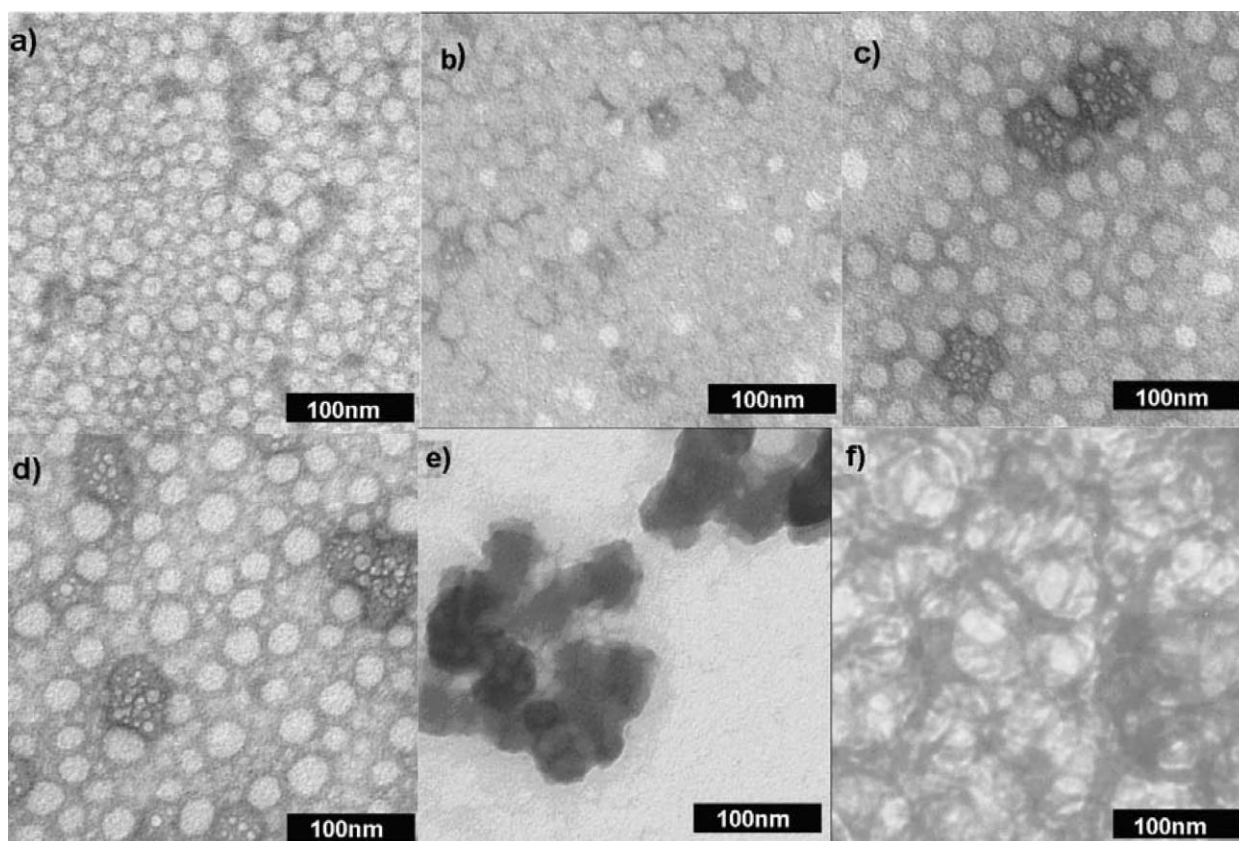
**Fig. 1** Transmission electron micrographs of (a) 0.5 wt% pentablock copolymer micelles in deionized water, (b) 0.5 wt% pentablock copolymer micelles in pH 3.0 calcium phosphate—aged 30 min, (c) 0.5 wt% pentablock copolymer micelles in pH 3.0 calcium phosphate—aged 1 hour, and (d, e) different regions of 0.5 wt% pentablock copolymer micelles in pH 3.0 calcium phosphate—aged 24 hours; (f) 30 wt% pentablock copolymer–pH 1.0 calcium phosphate gel.

micelles is shown in Fig. 1a. The micrographs of the pH 3.0 micelle samples prepared in inorganic solutions and aged for different time periods are presented in Fig. 1b–e. They clearly show the growth of the calcium phosphate coating (dark regions) around some (but not all) of the micelles, with time. The two 24 h aged micrographs, Fig. 1d, e, are from different areas of the same sample. These images show single coated micelles as well as agglomerates of many. The pentablock gels prepared with the pH 1.0 calcium phosphate solution (Fig. 1f), clearly indicated aggregates of spheres. The cryo-frozen gel appeared as a concentrated matrix of $\sim 60$ nm diameter spheres. Similar results were obtained with the Pluronic® solutions and gels. While there was no obvious visible second phase in the gel micrograph (Fig. 1f), EDS analysis showed strong calcium and phosphorus signals. These could be attributed to the amorphous calcium and phosphate ions in solution, or the precipitation of an inorganic calcium phosphate phase in the gel. XRD, NMR and SAXS studies were conducted to investigate the structure of the inorganic phase as well as the composite gel.

SAXS analysis was performed to investigate the ordered superstructure of the polymer-based nanocomposites. As shown in Fig. 2, the self assembled Pluronic® copolymer gel with and without the calcium phosphate nanocomposites both at pH 1.0 and 3.0 has distinct diffraction peaks with $Q/Q^*$ ($Q^*$ is the first order peak position) of $\sqrt{3} : \sqrt{4} : \sqrt{8} : \sqrt{11} : \sqrt{12}$,

indicating that the system exhibits a face-centered cubic (FCC) structure. The Pluronic® with calcium phosphate at pH 1.0 has additional higher order peaks, which implies that the system is better ordered. In addition, the Pluronic® gel with and without inorganic phase at pH 3.0 showed a similar inter-particle distance, $D$ ($D = \sqrt{3}d_{111}$, where $d_{111} = \frac{2\pi}{Q^*}$). At pH 1.0, however, $D$ increases from 15.5 to 17.1 nm with the addition of calcium
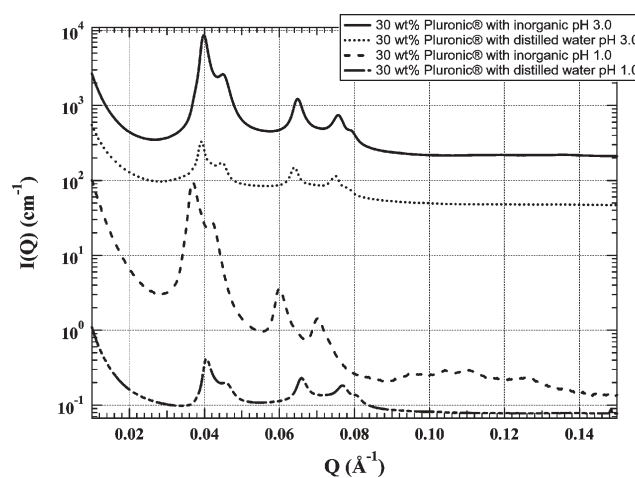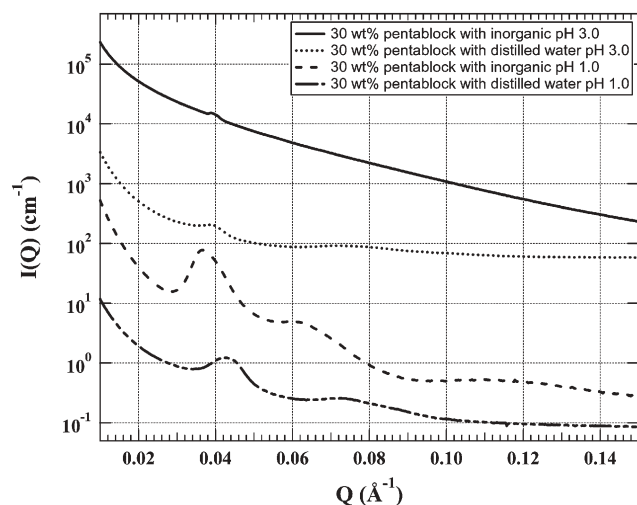


**Fig. 2** SAXS of Pluronic® F127 gels with and without calcium phosphate. Scattering patterns have been shifted vertically for clarity.

phosphate. This may be attributed to the different level of calcium phosphate precipitation over polymer micelles at different pH values. At pH 3.0, the precipitation rate of calcium phosphate is slow, the weight fraction of the inorganic phase is lower, as seen from TGA experiments (below) and only few micelles were coated with calcium phosphate, as seen in the TEM images. Due to the large number of micelles without inorganic coatings, the micelles coated with the calcium phosphate do not contribute much to the scattering. Hence, the *D* value remains similar in both Pluronic® gels with and without the inorganic phase at pH 3.0. At pH 1.0, the higher ionic concentration expedites the precipitation of calcium phosphate, and more micelles are coated with the inorganic phase. Thus, the micelle size increases due to the inorganic phase precipitation on the Pluronic®, causing an increase in *D*. This result is in agreement with the TEM data.

As for the pentablock copolymer gel nanocomposites in Fig. 3, few SAXS peaks are observed. Besides, the peaks are much broader than those for the Pluronic® gels, which means that the system is relatively poorly ordered. However, comparing the SAXS patterns of the Pluronic® and pentablock gels, the trends of the profiles are fairly consistent. Therefore, the morphology of pentablock gels with and without calcium phosphate may also exhibit FCC structure, and any broad peak has contributions from several peaks. For the pentablock copolymer gel with calcium phosphate at pH 3.0, no distinct higher order peaks were observed. This is presumably due to the formation of larger calcium phosphate particles in the interstitial spaces that disrupt the ordered pentablock copolymer packing structure. Compared to the *D* of the pure pentablock copolymer gel, there is a dramatic increase in *D* when the pentablock copolymer gels are coated with calcium phosphate at pH 1.0. This is consistent with the results seen with the Pluronic® gels with calcium phosphate at pH 1.0.
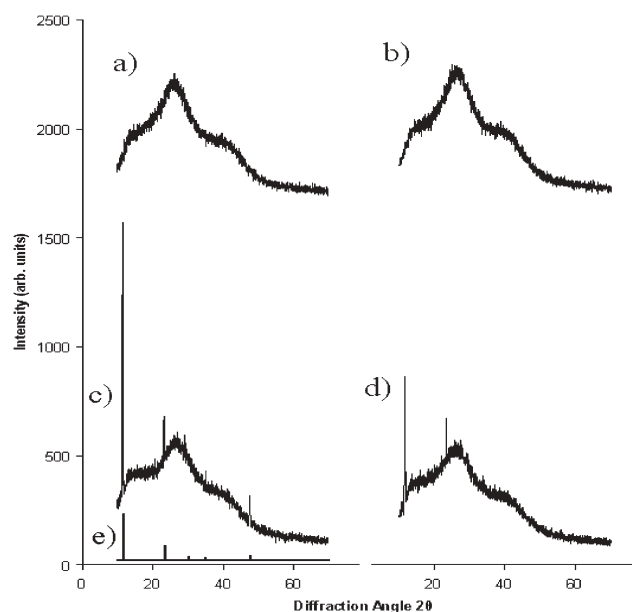
### Structure of the calcium phosphates

The initial precipitate formed upon mixing of the 0.5 M $Ca(NO_3)_2$ and $NH_4H_2PO_4$ aqueous solutions contained a mixture of synthetic brushite ($CaHPO_4 \cdot 2H_2O$) and monetite

($CaHPO_4$). XRD of the precipitate formed in the gel samples show a different inorganic phase. When precipitated on the copolymer gel template natural brushite, a mineral normally only found in caves,[13] was observed. One of the most common cave minerals, natural brushite forms in guano deposits at low pH and high phosphate rich solutions. Apparently, the copolymer gel template nicely mimics the process observed in Nature. Fig. 4 presents X-ray diffraction patterns of both the Pluronic® F127 and pentablock gels dissolved in deionized water and in the pH 3.0 calcium phosphate solution, as well as the characteristic peaks of natural brushite (ICDD card # 11-0293). Fig. 4a and b do not show any sharp peaks, but only amorphous reflections of the non-crystalline polymers. The pH 3.0 gel samples in Fig. 4c and d, however, show all five of natural Brushite's most intense peaks, compared with Fig. 4e. Using the Sherrer equation, we obtain brushite crystal sizes of >30 nm from the widths of the Bragg peaks.

Like the precipitate separated upon initial mixing of the calcium phosphate solutions, X-ray analysis of the higher ionic concentration pH 1.0 pentablock gel samples showed the synthetic brushite phase (Fig. 5a). Because the solution was much more concentrated, there was more of a driving force for precipitation on the polymer. This led to less controlled precipitation and formation of the inorganic phase. After drying for 24 hours in a desiccator, a second phase formed, identified as calcium dihydrogen phosphate (Fig. 5b). As the water evaporated from the sample, ions in solution were forced to precipitate. Because of the overwhelming driving force, ions precipitated heterogeneously as a second phase. Interestingly, this second phase was not present in the dried pH 1.0 Pluronic® F127 gel. The X-ray pattern of the dried Pluronic® F127 gel composite, Fig. 5c, showed two broad Bragg reflections. Similar peaks were observed in dried



Fig. 3 SAXS of pentablock copolymer gels with and without calcium phosphate. Scattering patterns have been shifted vertically for clarity.



Fig. 4 Wide-angle X-ray diffraction patterns of (a) 30 wt% pentablock in deionized water, (b) 30 wt% Pluronic® F127 in deionized water, (c) 30 wt% pentablock in pH 3.0 calcium phosphate solution, (d) 30 wt% Pluronic® F127 in pH 3.0 calcium phosphate solution, and (e) characteristic natural brushite peaks.
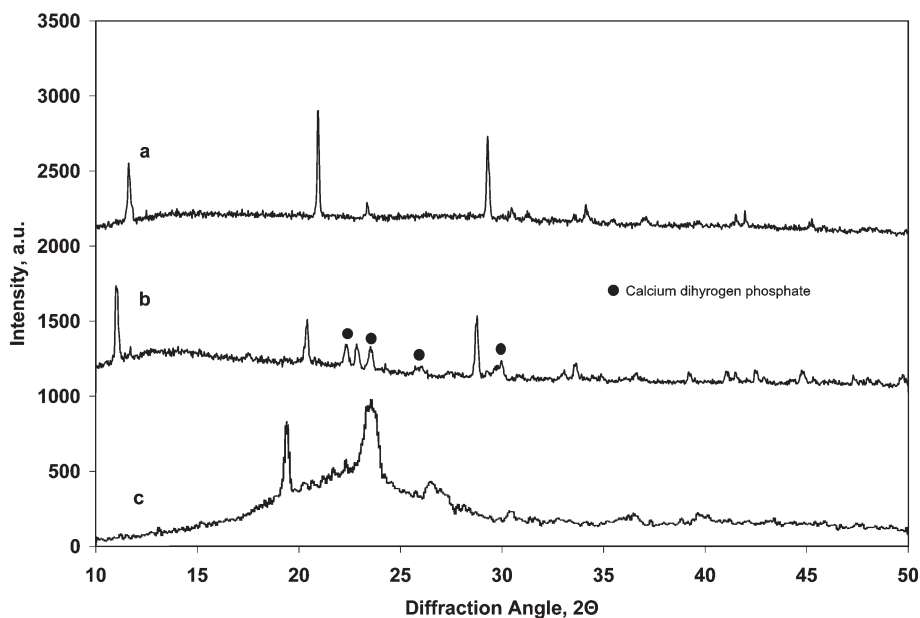
**Fig. 5** X-Ray diffraction patterns of (a) 30 wt% pentablock gel in pH 1.0 calcium phosphate solution, (b) same sample after 24 h drying in a desiccator and (c) dried Pluronic® F127 copolymer gel in pH 1.0 calcium phosphate solution.

Pluronic gel samples also indicating that they are due to crystallization of the PEO block upon drying. Nevertheless, the peak around $2\theta = 23°$ appears to be a composite peak including a band from calcium dihydrogen phosphate precipitate also. It was possible to control the amount of precipitation by adjusting the pH of the initial calcium phosphate solution as revealed by the TGA of the pH 3.0 and 1.0 samples illustrates this as shown in Fig. 6. After evaporating all the water out of the gel, a baseline weight was found for each sample. Because of the chemically-bound water from the brushite phase, water was not totally evaporated until the system reached 200 °C. At 400 °C, the polymer is burned off completely, leaving calcium phosphate residue
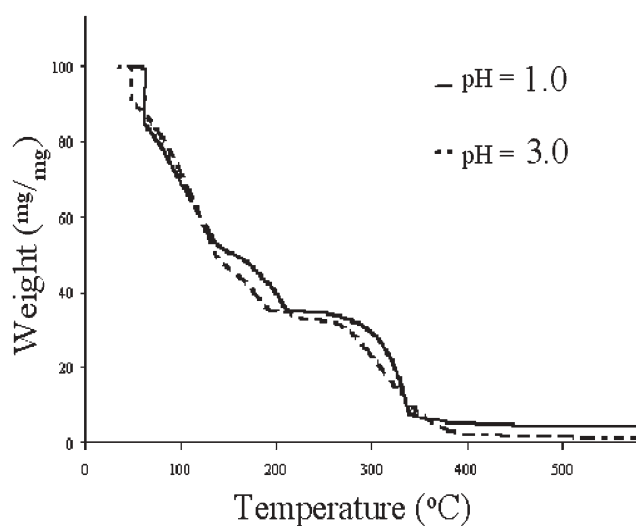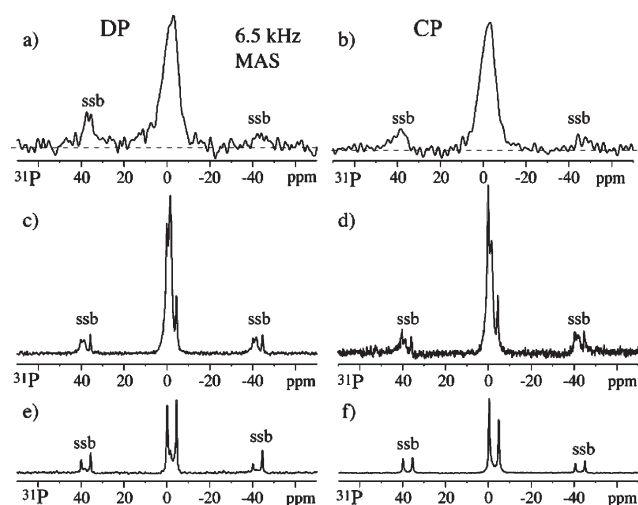
corresponding to 6.5% of the solid phase (after removal of water by ∼250 °C) in the pH 3.0 gel. As predicted by the pH solubility diagrams,[14] the inorganic weight% in the pH 1.0 gel sample was much higher at 15.0% (again, based on the mass of the dried gel at ∼250 °C). Using this data, it was also possible to calculate the initial concentrations of the calcium phosphate solutions. Assuming all of the left-over precipitate is the dehydrated monetite phase, it was determined that the initial calcium and phosphate concentrations were 0.5 M in the pH 1.0 and 0.2 M in the pH 3.0 calcium phosphate solutions. Considering the 40 mg size of the samples, these experimentally-calculated concentrations are consistent with the pH–concentration diagram of the calcium phosphate system.[14]

The composition of the phosphate can also be assessed by $^{31}P$ NMR. The $^{31}P$ NMR spectra of the dried Pluronic® F127– and pentablock–phosphate composites are shown in Fig. 7. Comparing the $^{1}H$–$^{31}P$ cross-polarization to the direct-polarization spectra, we see in both instances that the same peaks are present in both spectra, and with almost equal intensities for the Pluronic® F127–phosphate composite. This indicates that all the phosphates exist as protonated species. For the Pluronic® F127–phosphate, the resonance is indicative of monohydrogen phosphate ($CaHPO_4$) as found in brushite/monetite, while the pentablock phosphate contains a significant contribution (*ca.* 1/3 of all phosphate) from calcium dihydrogen phosphate ($Ca(H_2PO_4)_2$). For reference, the spectrum of pure $Ca(H_2PO_4)_2$ is shown in Fig. 7e, f; it exhibits two signals due to chemically inequivalent $H_2PO_4^-$ ions in the crystal structure. The Pluronic® F127–phosphate has a broader line shape as compared to the pentablock–phosphate, which suggests that the former exists in a more disordered environment. The spectra in Fig. 7a–d have been scaled to equal peak height, but the true integrals of the spectra in Fig. 7a and c indicate the presence of about five times more phosphate in the pentablock composite as compared to the



**Fig. 6** Thermogravimetric analysis of pH 1.0 and 3.0 for 30 wt% pentablock copolymer–calcium phosphate gel.

This journal is © The Royal Society of Chemistry 2007

*J. Mater. Chem.*, 2007, **17**, 1570–1578 | 1575

**Fig. 7** $^{31}$P NMR spectra of the dried (a, b) Pluronic® F127-phosphate composite (pH 1), (c, d) pentablock–phosphate composite (pH 1), and (e, f) calcium dihydrogen phosphate. The spectra were acquired with 6.5-kHz magic-angle spinning. Spinning sidebands are labelled "ssb". Direct-polarization (DP) spectra with (a) 400 s, (c) 1000 s, and (e) 100 s recycle delays are compared with 0.4-ms cross-polarization (CP) spectra in (b), (d), and (f).

Pluronic® F127 composite, given the almost equal fill factor in both sample rotors.

Furthermore, the $Ca(H_2PO_4)_2$ has a roughly twice longer $^{31}$P longitudinal ($T_1$) relaxation time as compared to the $CaHPO_4$, which indicates that there is no efficient $^{31}$P spin diffusion between the two phosphates on the 1-s time scale. This in turn means that the two phases are not in contact with domains on the 2-nm scale.

The $^1$H proton spectra of the Pluronic® F127 composite are shown in Fig. 8. The sharp resonances from the Pluronic® protons dominate the spectrum in the pentablock composite as well. Normally, in organic solid the proton resonances are very broad due to the strong multi-spin $^1$H–$^1$H dipolar couplings. However, fast segmental motion far above the glass transition average out the dipolar interactions in the Pluronic® F127 copolymer, resulting in the sharp lines seen in Fig. 8. The proton spectrum of the Pluronic® F127 composite shows a broad component (Fig. 8c, d), which may be due to the reduced mobility of the Pluronic® F127 segments near the brushite particles.

### Phosphate–polymer proximity

$^1$H–$^{31}$P WISE with $^1$H spin diffusion proved useful for characterizing the proximity of the inorganic components to the organic matrix. As seen in the WISE spectra of Fig. 9, for the Pluronic® F127 composite, $^1$H spin diffusion from the Pluronic® F127 to the brushite protons occurs within 50 ms of spin diffusion time, as proved by the characteristic sharp doublet of the Pluronic® F127 protons clearly visible after 50 ms of spin diffusion. Given a spin diffusion coefficient of $<0.5$ nm$^2$ ms$^{-1}$ in protonated phosphates, this indicates domain sizes of less than 20 nm. In contrast, there is hardly any evidence of spin diffusion contact in the case of the pentablock composite, see Fig. 10. After 50 ms of spin
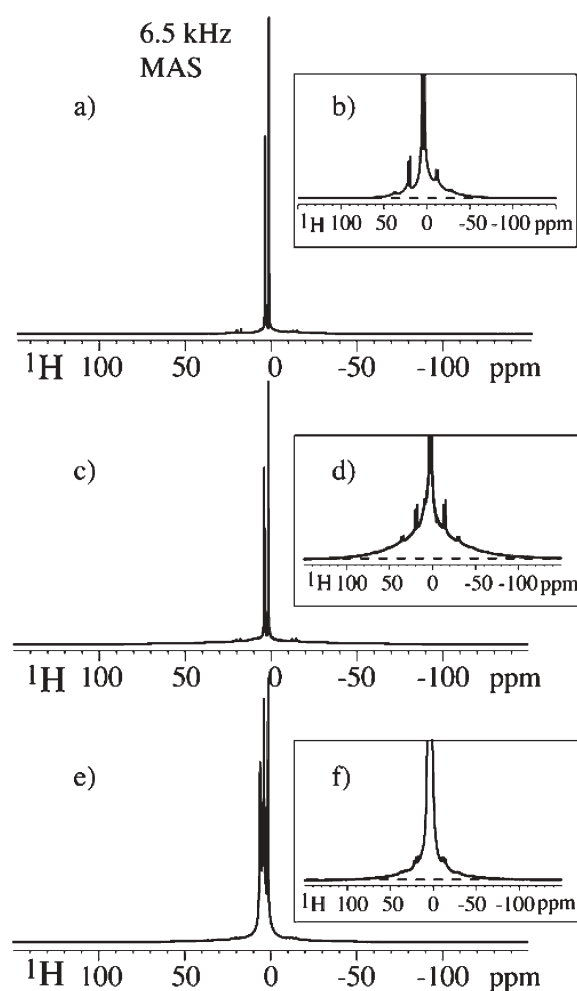


**Fig. 8** $^1$H NMR spectra of (a, b) the pure Pluronic® F127, (c, d) the Pluronic® F127–phosphate composite, and (e, f) the pentablock–phosphate composite at 6.5 kHz MAS. The insets (b), (d), and (f) focus in on the base of their respective spectra, revealing a broadened base of the pluronic®–phosphate composite.

diffusion, little line-shape change is observed, see Fig. 10 b, e. The characteristic doublet of the Pluronic® F127 block is absent. Only a minor signal in the 1–8 ppm range might be attributed to the polymer protons. This indicates large particles $>20$ nm in diameter, where most of the protons are far away from the pentablock copolymer matrix. No signs of spin diffusion, only signal reductions by $^1$H $T_1$ relaxation, are observed after 500 ms, see Fig. 10 c, f. This is completely consistent with the crystallite size of $>30$ nm estimated from the FWHM of the Bragg peaks of this sample, see above.

Based on the observations presented above, we propose that calcium phosphate nucleation occurs on the pentablock copolymer micelle surface, aided by the cationic characteristics of the PDEAEM end groups. This is clearly seen in the TEM images of the copolymer solutions at lower concentrations. As micelles, these hydrophilic end groups align themselves into a continuous cationic spherical surface. This attracts the ions in solution and provides sites for nucleation. A similar mechanism provides nucleation sites in the Pluronic® F127 gel. Pluronic® F127 micelles have polar OH end groups that,
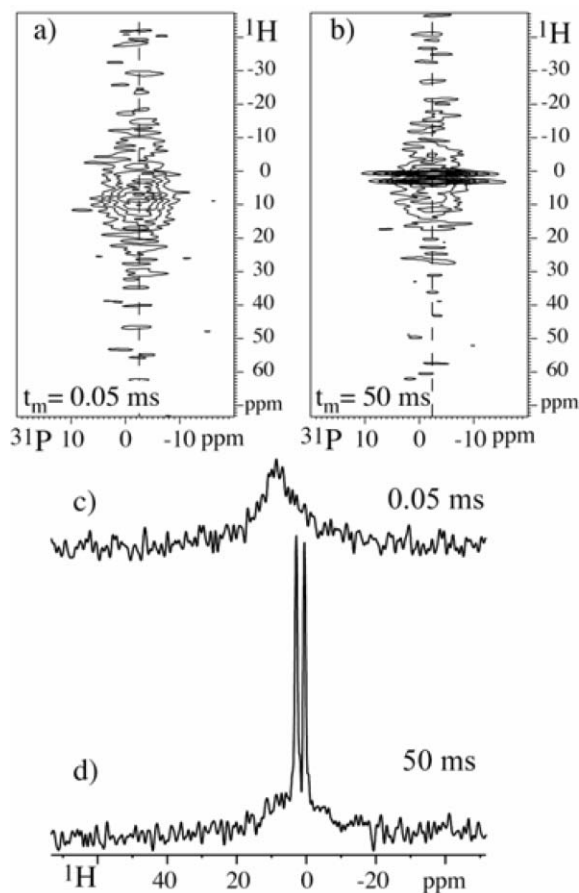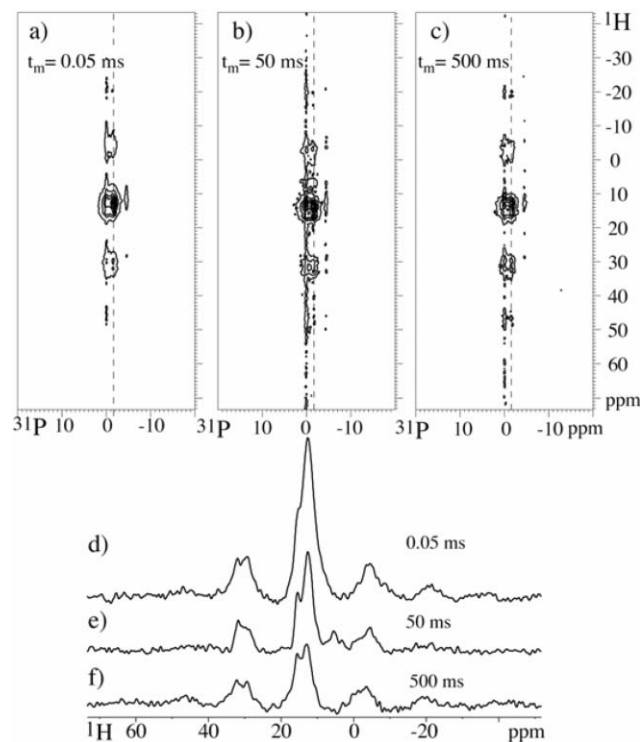
**Fig. 9** $^1H\{^{31}P\}$ 2D WISE with $^1H$ spin diffusion, at 6.5 kHz MAS, of the dried Pluronic® F127–phosphate composite; (a) and (b) are 2D contour plots of spectra recorded after 0.05 and 50 ms of spin diffusion, respectively. Fig. (c) and (d) are slices along the $^1H$ dimension extracted at −1.6 ppm in the $^{31}P$ dimension from the spectra in (a) and (b), respectively.



**Fig. 10** $^1H\{^{31}P\}$ 2D WISE with $^1H$ spin diffusion, at 6.5 kHz MAS, of the dried pentablock–phosphate composite (pH 1.0, 30 wt% copolymer, calcium phosphate). (a), (b) and (c), are 2D contour plots of spectra recorded after 50 μs, 50 ms and 500 ms of spin diffusion respectively. Fig. (d), (e) and (f) are slices extracted along the $^1H$ dimension from (a), (b), and (c), respectively, indicated by the dashed lines corresponding to 1.6 ppm in the $^{31}P$ dimension. The bands flanking the main peak on either side, labelled ssb, are spinning sidebands, mostly due to the large chemical-shift anisotropy of –OH protons.

when assembled as a surface, can provide slightly negatively-charged sites for nucleation. Because of the high concentration of polymer in the gel samples, at temperatures above 5 °C the micelles with the inorganic coatings agglomerate into nanocomposite networks with ordered structures.

## Conclusions

In this work, we have successfully demonstrated the formation of macroscale polymer–inorganic nanocomposite solids with ordered micro- and nanostructures completely by self-assembly in solution. By changing the ionic character of copolymer micelles in solution, we can vary the formation and composition of the inorganic phase on copolymer micelles in aqueous solutions. Appropriate copolymer design and synthesis and the use of gel-forming self-assembling copolymers, makes possible the formation of macro-sized ordered networks of spherical nanocomposites for a bottom-up approach to materials design, while most previous work has focused on mineralizing the surface of bulk polymers[4–6] or forming sub-micron aggregates of organic–inorganic nanocomposites.[7,15] The nanocomposites formed were characterized by electron microscopy, X-ray scattering, and advanced solid-state NMR. XRD and $^{31}P$ 1-D

NMR identified the phosphate in the Pluronic® F127 composite as a disordered brushite type species, while the inorganic calcium phosphate phase in the pentablock composite is relatively more ordered and contains ∼25% crystalline calcium dihydrogen phosphate that forms during drying. TGA and NMR showed that there is a higher mineral content in the pentablock composite as compared to the Pluronic® F127 composite. $^1H$–$^{31}P$ WISE NMR experiments with $^1H$ spin diffusion indicated that the brushite particles in the Pluronic® matrix are <15 nm in diameter, while NMR and analysis of peak widths in XRD showed that the brushite and calcium dihydrogen phosphate particles in the pentablock system are significantly larger (>30 nm). The ability to form a nanocrystalline calcium phosphate phase from aqueous solutions onto self-assembling copolymer micelles and gels is a first step in mimicking the mineralization of collagen in bone formation. It is believed that insight into the nucleation and growth of calcium phosphate on polymer surfaces will lead to a better understanding of bone formation, and design of better bone implants.

## Acknowledgements

## References

1 A. Malsy and M. Bohner, Brushite conversion into apatite, *Eur. Cells Mater.*, 2005, **10**(1), 28.

2 L. Jonasova, F. A. Muller, A. Helebrant, J. Strnad and P. Greil, Hydroxyapatite formation on alkali-treated titanium with different content of $Na^+$ in the surface layer, *Biomaterials*, 2002, **23**(15), 3095–3101.

3 L. Jonasova, F. A. Muller, A. Helebrant, J. Strnad and P. Greil, Biomimetic apatite formation on chemically treated titanium, *Biomaterials*, 2004, **25**(7–8), 1187–1194.

4 F. A. Muller, *et al.*, Biomimetic apatite formation on chemically modified cellulose templates, in *The Annual Meeting of the International Society for Ceramics in Medicine, Nov. 6–9 2003*, 2004, Porto, Portugal, Trans Tech Publications Ltd.

5 J. Song, E. Saiz and C. R. Bertozzi, A new approach to mineralization of biocompatible hydrogel scaffolds: an efficient process toward 3-dimensional bonelike composites, *J. Am. Chem. Soc.*, 2003, **125**(5), 1236–1243.

6 J. Song, E. Saiz and C. R. Bertozzi, Preparation of pHEMA–CP composites with high interfacial adhesion *via* template-driven mineralization, *J. Eur. Ceram. Soc.*, 2003, **23**(15), 2905–2919.

7 V. M. Rusu, C. Ng, M. Wilke, B. Tiersch, P. Fratzi and M. G. Peter, Size-controlled hydroxyapatite nanoparticles as self-organized organic–inorganic composite materials, *Biomaterials*, 2005, **26**(26), 5414–5426.

8 M. D. Determan, J. P. Cox, S. Seifert, P. Thiyagarajan and S. K. Mallapragada, Synthesis and characterization of temperature and pH-responsive pentablock copolymers, *Polymer*, 2005, **46**(18), 6933–6946.

9 M. D. Determan, J. P. Cox and S. K. Mallapragada, Drug release from pH-responsive thermogelling pentablock copolymers, *J. Biomed. Mater. Res.*, in press.

10 Q. Chen, S. S. Hou and K. Schmidt-Rohr, A simple scheme for probehead background suppression in one-pulse ^{1}H NMR, *Solid State Nucl. Magn. Reson.*, 2004, **26**(1), 11–15.

11 K. Schmidt-Rohr, J. Clauss and H. W. Spiess, Correlation of structure, mobility, and morphology information in heterogeneous polymer materials by two-dimensional wideline-separation NMR spectroscopy, *Macromolecules*, 1992, **25**(12), 3273–3277.

12 S. S. Hou, F. L. Beyer and K. Schmidt-Rohr, High-sensitivity multinuclear NMR spectroscopy of a smectite clay and of clay-intercalated polymer, *Solid State Nucl. Magn. Reson.*, 2002, **22**(2–3), 110–127.

13 J. W. Murray and R. V. Dietrich, Brushite and taranakite from Pig Hole Cave, Giles County, Virginia, *Am. Mineral.*, 1956, **41**, 616–26.

14 H. Oonishi and K. Oomamiuda, Degradation/resorption in bioactive ceramics in orthopaedics, *Handbook of Biomaterial Properties, First edn*, ed. J. Black and G. Hastings, 1998, Chapman and Hall, London, p. 590.

15 Y. F. Zhao and J. Ma, Triblock co-polymer templating synthesis of mesostructured hydroxyapatite, *Microporous Mesoporous Mater.*, 2005, **87**(2), 110–117.